Plasmon-Enhanced Photoemission from a Single $Y_3N@C_{80}$ Fullerene†

Palash Bharadwaj and Lukas Novotny*

Institute of Optics and Department of Physics and Astronomy, University of Rochester, Rochester, New York 14627

Received: November 25, 2009; Revised Manuscript Received: January 18, 2010

Rare earth ions are the backbone of a wide range of optoelectronic applications, ranging from solid-state lasers and fiber amplifiers to silicon photonics. So far experiments on single rare-earth ions have been elusive because of the long excited state lifetimes and low absorption cross sections. Here we present the first single molecule photoemission study of an endohedral metallofullerene ($Y_3N@C_{80}$). This molecule has a low intrinsic photoluminescence quantum yield and a long radiative lifetime. We find that the Y_3N species is rigidly attached to the C_{80} cage, imparting a fixed absorption dipole moment to the molecule as a whole. To improve the absorption and emission of light, we couple single $Y_3N@C_{80}$ molecules to single gold nanoparticles, which results in a photoluminescence enhancement of 2 orders of magnitude. Such unexpectedly high enhancements are a consequence of the low intrinsic quantum yield of $Y_3N@C_{80}$. Our work paves the way for applications of rare-earth ions on the single emitter level.

Introduction

$Y_3N@C_{80}$ are a member of the larger family of endohedral metallofullerenes.[1,2] The $Y_3N@C_{80}$ molecule consists of three yttrium and one nitrogen ion (Y_3N) encapsulated inside a C_{80} fullerene. These molecules, which do not exist naturally, are stabilized by a transfer of 6 electrons from yttrium nitride to the C_{80} cage.[1] To date, rare earth ions such as yttrium could not be observed on the single ion level, which is due to their long excited state lifetime and their low absorption cross-section. Here we demonstrate that photoluminescence from fullerene-incarcerated yttrium ions ($Y_3N@C_{80}$) can be readily detected and imaged when coupled to a single gold nanoparticle.

The gold nanoparticle acts as an optical antenna. It effectively converts propagating optical radiation to localized energy, and vice versa.[3] Noble metal nanoparticles (Au, Ag) offer a feasible bottom-up realization of optical antennas because of their localized surface plasmon resonances in the visible. Such antennas are particularly well suited for single emitter photoluminescence (PL) studies because, unlike extended sharp metallic tips, nanoparticles do not support the propagating surface plasmons that can lead to severe PL quenching.[4] Nanoparticles therefore offer a trade-off between desirable high field enhancement and undesirable nonradiative losses (quenching). PL enhancements of 1 order of magnitude using gold and silver particle antennas have been reported in recent years,[5,6] establishing such antennas as a controllable and reproducible choice for high-resolution PL imaging.[7] The highest PL enhancements occur for emission wavelengths slightly red-shifted from the localized plasmon resonance of the antenna. This finding has its origin in the different spectral dependences of the excitation rate and nonradiative energy transfer rate to the antenna.[8]

An optical antenna influences the excitation rate Γ_{exc} of an emitter as well as its quantum yield Q. Because the intrinsic quantum yield of good emitters is near unity, an optical antenna only decreases the quantum yield.[6] On the other hand, for poor emitters the antenna boosts both the excitation rate and the quantum yield, resulting in much higher net PL enhancements as compared to good emitters.[9,10] In this work we demonstrate PL enhancements of ~100 for an yttrium nitride cluster encaged in a C_{80} fullerene.

Confocal Studies of Single $Y_3N@C_{80}$ Fullerenes

A schematic of the structure of a $Y_3N@C_{80}$ molecule is shown in Figure 1a. $Y_3N@C_{80}$ has been reported in literature to have an absorption onset around 750 nm, corresponding to the first singlet $(HOMO\rightarrow LUMO)_0$ transition. It also has a strong absorption peak around 639 nm which is attributed to the $(HOMO\rightarrow LUMO)_2$ transition.[11] A simplified energy level scheme for $Y_3N@C_{80}$ is shown in Figure 1b (not all levels shown).[11] From density functional studies, the highest occupied molecular orbital (HOMO) is expected to be localized on the C_{80} while the lowest unoccupied molecular orbital (LUMO) is primarily on the yttrium nitride.[12] Light absorption in $Y_3N@C_{80}$ is therefore dominated by the cage, while light emission (photoluminescence) arises predominantly from the yttrium nitride cluster. In our experiments, we excite the $(HOMO\rightarrow LUMO)_2$ transition with a 635 nm laser and collect the PL from the $(HOMO\rightarrow LUMO)_0$ transition using a band-pass filter centered around 700 nm.

Figure 1c shows the PL spectrum of $Y_3N@C_{80}$ in xylene excited at 633 nm. The spectrum is characterized by the $(HOMO\rightarrow LUMO)_0$ emission, represented by a peak centered around 710 nm. The lifetime of this transition has been determined by a pulsed laser source with center wavelength 625 nm. The resulting emission decay profile is shown in Figure 1d revealing a lifetime of 240 ns. While this may appear long compared to the lifetime of typical organic dyes (few ns), it is surprisingly short compared to the lifetime of typical rare-earth metal ions (Er^{3+}, Yb^{3+}, Y^{3+}, and so forth) in solid state hosts, which is typically in the range of microseconds to milliseconds. This drastic reduction in lifetime is due to efficient electronic or vibrational coupling between Y_3N and C_{80}.[13,14]

To perform measurements on single $Y_3N@C_{80}$ molecules we first prepared a dilute solution and then deposited $Y_3N@C_{80}$ on

† Part of the "Martin Moskovits Festschrift".

* To whom correspondence should be addressed. E-mail: novotny@optics.rochester.edu.

10.1021/jp911226p
Published on Web 03/01/2010

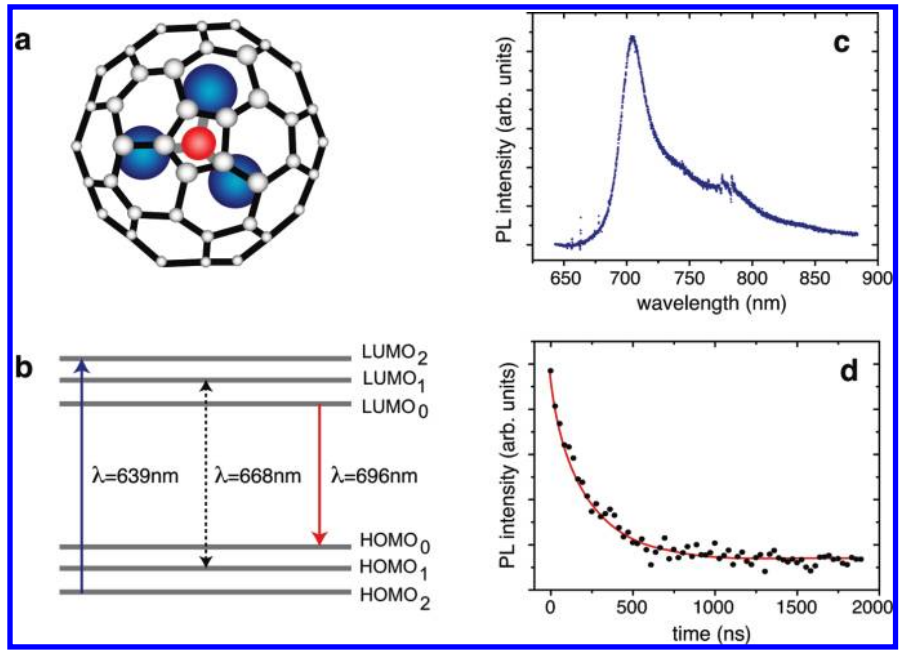

Figure 1. (a) Schematic representation of the $Y_3N@C_{80}$ molecule consisting of a Y_3N ion incarcerated inside a C_{80} cage. The blue spheres denote the yttrium ions while the red sphere represents a nitrogen ion. (b) Energy level structure for $Y_3N@C_{80}$. (c) Photoluminescence spectrum of $Y_3N@C_{80}$ molecules in solution upon excitation at 633 nm. The kinks originate from the subtraction of the solvent Raman spectrum. (d) Lifetime measurement for the transition centered around 710 nm. The decay is well-fit by a single exponential yielding a lifetime of 240 ns ± 10 ns.

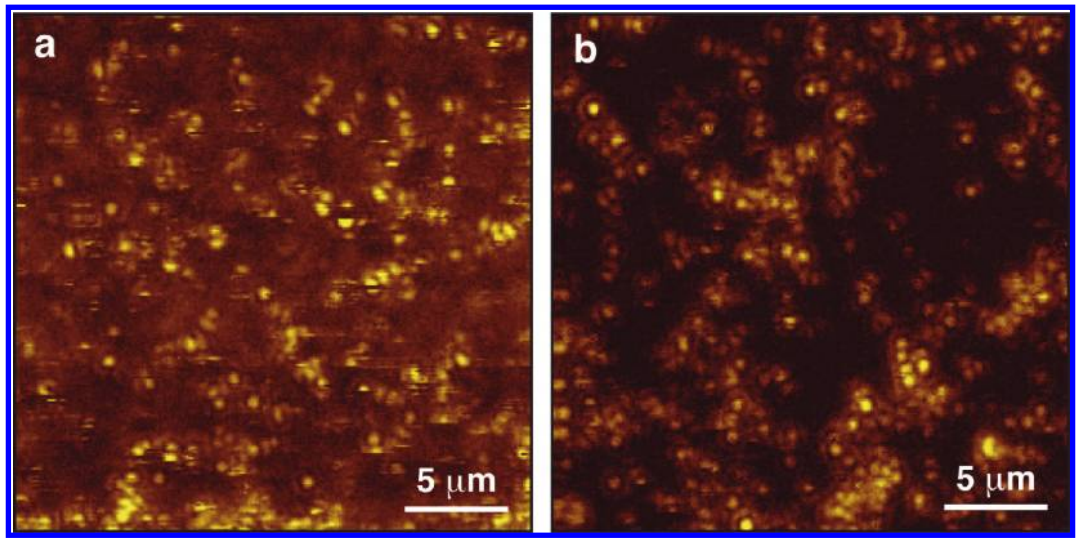

Figure 2. Confocal photoluminescence images of single (a) $Y_3N@C_{80}$ molecules and (b) nile blue molecules. The excitation intensities are 60 kW/cm^2 for $Y_3N@C_{80}$ and 2 kW/cm^2 for nile blue. Typical photoluminescence counts for $Y_3N@C_{80}$ are around 7−8 kHz and for nile blue around 30 kHz.

a transparent surface by spin coating. The photophysical properties of the Y-trimetaspheres were found to be very sensitive to the local dielectric environment. For example, on mica or on a clean glass surface, only a tiny fraction of the $Y_3N@C_{80}$ gave any detectable fluorescence, and even that was marred by severe blinking. This is not surprising given that both mica and clean glass have a negatively charged surface, as does the C_{80} shell of $Y_3N@C_{80}$. On the other hand, best results were obtained when the $Y_3N@C_{80}$ were placed on top of a thin layer of poly(methyl methacrylate) (PMMA); however, even then, significant molecule-to-molecule variations were noticed. Some molecules, apparently residing in "sweet spots" in the PMMA, were remarkably photostable, while others blinked or photobleached. Therefore, all further studies used ∼10 nm PMMA spincoated on a glass coverslip as the substrate of choice. Figure 2a shows a confocal PL image of single $Y_3N@C_{80}$ molecules excited with a radially polarized laser beam with wavelength λ = 635 nm. The image reveals typical dipole-like absorption patterns[15] from which we infer that the metal nitride rotor is not free to rotate inside the C_{80} cage, but rather has a fixed, stable configuration.

To estimate the intrinsic PL quantum yield (Q_i) of $Y_3N@C_{80}$ we performed similar measurements on a reference sample with dispersed nile blue molecules (cf. Figure 2b). The molar absorptivity of $Y_3N@C_{80}$ at λ = 635 nm is determined to be ∼9000 M^{-1} cm^{-1} while for nile blue it is 80 000 M^{-1} cm^{-1}.[16] Consequently, knowing the quantum yield of nile blue (∼0.8), we can estimate the intrinsic quantum yield of $Y_3N@C_{80}$ to be Q_i <0.05. Therefore, the weak PL from $Y_3N@C_{80}$ is the result of both low absorption and a low quantum yield.

Photoemission Enhancement

We next demonstrate that the PL efficiency of $Y_3N@C_{80}$ can be enhanced by 2 orders of magnitude by coupling it to a gold

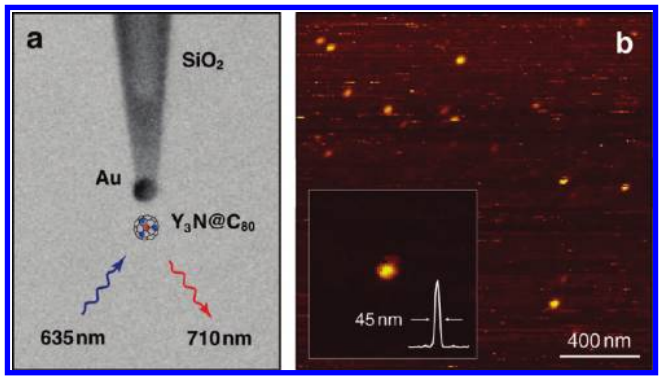

Figure 3. Antenna-coupled photoluminescence from single $Y_3N@C_{80}$ molecules. (a) SEM image of a gold nanoparticle antenna (80 nm diameter) with superimposed illustration of the experiment. (b) 2 μm $\times$ 2 μm photoluminescence image of $Y_3N@C_{80}$ recorded by raster scanning the sample underneath the nanoparticle antenna. Excitation intensity is 2 kW/cm^2 and the photoluminescence counts from the brightest molecules is around 120 kHz. Without antenna the photoluminescence count rate drops to 1 kHz. Inset of (b): zoomed-in image of one of the bright spots.

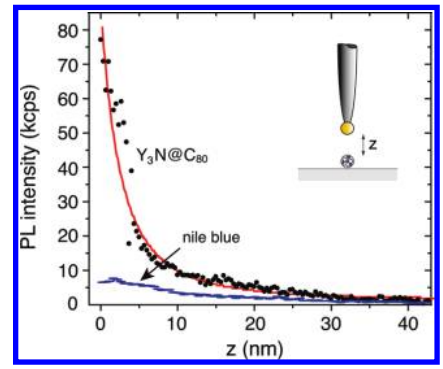

Figure 4. Photoluminescence from a single $Y_3N@C_{80}$ molecule as a function of separation between molecule and gold nanoparticle. At short separations the nanoparticle antenna enhances the photoluminescence by a factor of $\sim$100. For a single nile blue molecule the enhancement is in the range of 8$-$10. Dots are experimental data and the solid line is a fit according to a dipole model.

nanoparticle. The nanoparticle acts as a simple optical antenna that increases the local excitation field and boosts the low quantum yield of $Y_3N@C_{80}$. The PL increase of 2 orders of magnitude makes the antenna-coupled $Y_3N@C_{80}$ as efficient as ordinary dye molecules.

In free space and for excitation intensities below saturation, the PL rate Γ^o_{fl} of a single $Y_3N@C_{80}$ molecule can be written as[8]

$$\Gamma^o_{fl} = \Gamma^o_{exc} \cdot Q_i = \Gamma^o_{exc} \frac{\Gamma^o_{rad}}{\Gamma^o_{rad} + \Gamma^o_{nr}} \quad (1)$$

where Γ_{exc} is the excitation rate, and Q_i is the intrinsic quantum yield of the emitter defined in terms of the intrinsic radiative rate and nonradiative relaxation rate (Γ^o_{rad} and Γ^o_{nr}). The gold nanoparticle increases Γ_{exc} due to local field enhancement, and by reciprocity, this increase is roughly matched by an increase in Γ_{rad}.[3] However, the antenna also absorbs energy from the emitter and leads to an increase in the nonradiative relaxation rate Γ_{nr} (quenching).[17,18] For good emitters, which have $Q_i \approx 1$, it is not possible to increase the quantum yield further.[6] On the other hand, when $Q_i \ll 1$, as is the case of $Y_3N@C_{80}$, it is possible to increase the quantum yield by coupling the emitter to an optical antenna, such as a gold nanoparticle.[3] Thus, the antenna boosts both the excitation rate and the quantum yield in poor emitters, resulting in much higher net PL enhancements as compared to good emitters.[9,10]

To validate these predictions we attach a single 80 nm gold nanoparticle to the end of a glass tip[19] and position it by using standard tuning-fork based control[6] over the sample with dispersed $Y_3N@C_{80}$ molecules. This system is also used to raster scan the nanoparticle antenna over the sample surface while maintaining a constant particle-sample distance (typically $\sim$5 nm). Figure 3a shows a scanning electron micrograph (SEM) of a typical gold nanoparticle antenna with a superimposed sketch of the experimental configuration. A high numerical aperture objective is used for exciting single $Y_3N@C_{80}$ molecules at a wavelength of $\lambda = 635$ nm and for collecting the emitted photoluminescence centered around $\lambda = 710$ nm. PL photons are detected by a single photon counting avalanche photodiode. A representative near-field PL map is shown in Figure 3b. Each of the bright spots in this figure corresponds to a single $Y_3N@C_{80}$ molecule. The single molecule nature of these spots is confirmed by the intermittent blinking events. During image acquisition, individual $Y_3N@C_{80}$ molecules tend to attach themselves to the gold nanoparticle, which gives rise to random bright spots and streaks seen across the near-field PL map.

We next examine the dependence of the PL enhancement on the separation between a single $Y_3N@C_{80}$ molecule and the gold nanoparticle. For this purpose, we center the nanoparticle antenna over a single $Y_3N@C_{80}$ molecule and record the PL as a function of separation z. The experimental results are shown in Figure 4 together with calculations based on a simple dipole model.[8] For comparison, similar measurements were performed for a single nile blue molecule and the results are included in Figure 4. For $Y_3N@C_{80}$ we observe a PL enhancement of $\sim$100 whereas for nile blue the enhancement is only 8$-$10, consistent with previous observations.[6] The giant PL enhancement of $Y_3N@C_{80}$ cannot be explained by an increase in the excitation rate Γ_{exc} alone, but is instead the consequence of both an increase in the excitation rate and the low intrinsic quantum yield of the molecule. From the measured distance-dependent PL rate we estimate the intrinsic quantum yield of Y-TMS to be $Q_i \sim 0.02$ which is close to our estimate based on confocal measurements. Interestingly, we do not observe any quenching from $Y_3N@C_{80}$ even as the antenna appears to touch the PMMA surface (cf. Figure 4). Note that this reduction in quenching zone for low Q_i molecules compared to good emitters (like nile blue) is expected and results from the interplay between Γ_{exc}, Γ_r, and Γ_{nr} for short antenna-molecule distances.[3] In contrast to a good emitter whose quantum yield drops monotonically as the antenna comes closer, the quantum yield of molecules such as $Y_3N@C_{80}$ is enhanced in the distance range of 5$-$20 nm, thereby pushing the onset of net quenching down to very short distances (<2 nm). This regime is inaccessible in our experiments because the most photostable $Y_3N@C_{80}$ molecules are most likely inside nanoscale holes or depressions of the PMMA film.

Conclusions

Our findings indicate that optical antennas can be employed to drastically enhance light absorption and emission from poor emitters like rare-earth ions. The observed photoluminescence enhancement of 2 orders of magnitude makes a single yttrium nitride molecule as efficient as a typical dye molecule. The PL enhancement can be further improved by optimized antenna

geometries, such as gold nanorods acting as optical half-wave antennas,[3] gap antennas,[20,21] bow-tie antennas,[22−24] or multielement antennas.[25] Our results have implications not only for improving the efficiency of a novel class of photovoltaic devices based on endohedral metallofullerenes[26] but also for enhancing the photoemission from low efficiency systems, such as nanocrystalline silicon or organic light emitting devices (OLEDs). Furthermore, the possibility of observing and controlling the photoemission from a single yttrium nitride molecule opens the door for optoelectronic applications on the single rare-earth ion level, ranging from single photon sources to biosensing.

Acknowledgment. The authors thank Luna Innovations, Inc. for the $Y_3N@C_{80}$ sample. They are grateful to Brian Holloway, Omar Torrens, and Martin Drees for valuable suggestions and discussions. They also acknowledge help from John Lesoine, Gustavo Cancado, and Prahnesh Venkataraman in sample characterization. This work was funded by the U.S. Department of Energy (DE-FG02-01ER15204).

References and Notes

(1) Stevenson, S.; Rice, G.; Glass, T.; Harich, K.; Cromer, F.; Jordan, M. R.; Craft, J.; Hajdu, E.; Bible, R.; Olmstead, M. M.; Maitra, K.; Fisher, A. J.; Balch, A. L.; Dorn, H. C. *Nature* **1999**, *401*, 55–57.

(2) Dunsch, L.; Yang, S. *Phys. Chem. Chem. Phys.* **2007**, *9*, 3067–3081.

(3) Bharadwaj, P.; Deutsch, B.; Novotny, L. *Adv. Opt. Phot.* **2009**, *1*, 438–483.

(4) Issa, N. A.; Guckenberger, R. *Opt. Express* **2007**, *15*, 12131–12144.

(5) Kühn, S.; Hakanson, U.; Rogobete, L.; Sandoghdar, V. *Phys. Rev. Lett.* **2006**, *97*, 017402.

(6) Anger, P.; Bharadwaj, P.; Novotny, L. *Phys. Rev. Lett.* **2006**, *96*, 113002.

(7) Höppener, C.; Novotny, L. *Nano Lett.* **2008**, *8*, 642–646.

(8) Bharadwaj, P.; Novotny, L. *Opt. Express* **2007**, *15*, 14266–14274.

(9) Wokaun, A.; Lutz, H.-P.; King, A. P.; Wild, U. P.; Ernst, R. R. *J. Chem. Phys.* **1983**, *79*, 509–514.

(10) Tam, F.; Goodrich, G. P.; Johnson, B. R.; Halas, N. J. *Nano Lett.* **2007**, *7*, 496–501.

(11) Dunsch, L.; Krause, M.; Noack, J.; Georgi, P. *J. Phys. Chem. Solids* **2004**, *65*, 309–315.

(12) Valencia, R.; Rodriguez-Fortea, A.; Clotet, A.; de Graaf, C.; Chaur, M. N.; Echegoyen, L.; Poblet, J. M. *Chem.—Eur. J.* **2008**, *455*, 376–378.

(13) Zhu, W.; Agrawal, A.; Nahata, A. *Chem. Phys. Lett.* **2008**, *461*, 285–289.

(14) Dantelle, G.; Tiwari, A.; Rahman, R.; Plant, S. R.; Porfyrakis, K.; Mortier, M.; Taylor, R. A.; Briggs, G. A. D. *Opt. Mater.* **2009**, *32*, 251−256.

(15) Novotny, L.; Beversluis, M. R.; Youngworth, K. S.; Brown, T. G. *Phys. Rev. Lett.* **2001**, *86*, 5251.

(16) Douhal, A. *J. Phys. Chem.* **1994**, *98*, 13131–13137.

(17) Kuhn, H. *J. Chem. Phys.* **1970**, *53*, 101–108.

(18) Thomas, M.; Greffet, J.-J.; Carminati, R.; Arias-Gonzalez, J. R. *Appl. Phys. Lett.* **2004**, *85*, 3863.

(19) Kalkbrenner, T.; Ramstein, M.; Mlynek, J.; Sandoghdar, V. *J. Microsc.* **2001**, *202*, 72–76.

(20) Mühlschlegel, P.; Eisler, H.-J.; Martin, O. J. F.; Hecht, B.; Pohl, D. W. *Science* **2005**, *308*, 1607.

(21) Ghenuche, P.; Cherukulappurath, S.; Taminiau, T. H.; van Hulst, N. F.; Quidant, R. *Phys. Rev. Lett.* **2008**, *101*, 116805.

(22) Kinkhabwala, A.; Yu, Z.; Fan, S.; Avlasevich, Y.; Müllen, K.; Moerner, W. E. *Nat. Photonics* **2009**, *3*, 654–657.

(23) Farahani, J. N.; Pohl, D. W.; Eisler, H.-J.; Hecht, B. *Phys. Rev. Lett.* **2005**, *95*, 017402.

(24) Schuck, P.; Fromm, D. P.; Sundaramurthy, A.; Kino, G. S.; Moerner, W. E. *Phys. Rev. Lett.* **2005**, *94*, 017402.

(25) Taminiau, T. H.; Stefani, F. D.; van Hulst, N. F. *Opt. Express* **2008**, *16*, 10858.

(26) Ross, R. B.; Cardona, C. M.; Guldi, D. M.; Sankaranarayanan, S. G.; Reese, M. O.; Kopidakis, N.; Peet, J.; Walker, B.; Bazan, G. C.; Keuren, E. V.; Holloway, B. C.; Drees, M. *Nat. Mater.* **2009**, *8*, 208–212.

JP911226P